Cancer Pathogenesis and Therapy 3 (2025) 48–59

Contents lists available at ScienceDirect

Cancer Pathogenesis and Therapy

journal homepage: www.journals.elsevier.com/cancer-pathogenesis-and-therapy

Research article

# Integrative analysis of cuproptosis-related lncRNAs: Unveiling prognostic significance, immune microenvironment, and copper-induced mechanisms in prostate cancer☆

Haitao Zhong [a,b,c,1], Yiming Lai [a,b,c,d,1], Wenhao Ouyang [e,1], Yunfang Yu [e,f,1], Yongxin Wu [a,b,c], Xinxin He [g], Lexiang Zeng [a,b,c], Xueen Qiu [h], Peixian Chen [a,b,c], Lingfeng Li [a,b,c], Jie Zhou [a,b,c], Tianlong Luo [a,b,c], Hai Huang [a,b,c,i,*]

[a] Department of Urology, Sun Yat-sen Memorial Hospital, Sun Yat-sen University, Guangzhou, Guangdong 510120, China
[b] Guangdong Provincial Key Laboratory of Malignant Tumor Epigenetics and Gene Regulation, Sun Yat-sen Memorial Hospital, Sun Yat-sen University, Guangzhou, Guangdong 510120, China
[c] Guangdong Provincial Clinical Research Center for Urological Diseases, Sun Yat-sen Memorial Hospital, Sun Yat-sen University, Guangzhou, Guangdong 510120, China
[d] Department of Urology, The Fifth Affiliated Hospital of Xinjiang Medical University, Urumqi, Xinjiang 830011, China
[e] Department of Medical Oncology, Sun Yat-sen Memorial Hospital, Sun Yat-sen University, Guangzhou, Guangdong 510120, China
[f] Faculty of Medicine, Macau University of Science and Technology, Avenida WaiLong, Taipa, Macao 999078, China
[g] Department of Pathology, Sun Yat-sen Memorial Hospital, Sun Yat-sen University, Guangzhou, Guangdong 510120, China
[h] Department of Emergency, Sun Yat-sen Memorial Hospital, Sun Yat-sen University, Guangzhou, Guangdong 510120, China
[i] Department of Urology, The Sixth Affiliated Hospital of Guangzhou Medical University, Qingyuan People's Hospital, Qingyuan, Guangdong 511518, China

## HIGHLIGHTS

- Herein, we elucidate the prognostic value of cuproptosis-related long non-coding ribonucleic acid (lncRNA) in prostate cancer (PCa)
- Prognostic modeling was successfully established using a multi-level attention graph neural network (MLA-GNN)
- Cuproptosis-related lncRNA AC106820.5 could be a therapeutic target for PCa

## GRAPHICAL ABSTRACT

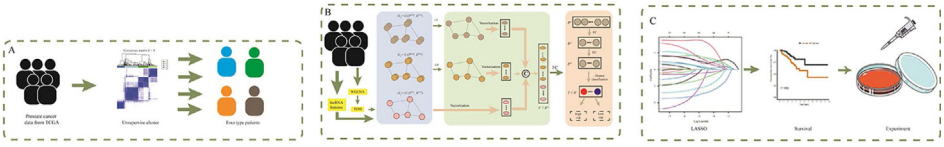

The workflow of the study. (A) We retrieved the expression data of cuproptosis-related lncRNAs and relevant clinical data from public databases for patients with prostate cancer. Based on the differential levels of gene expression, patients were divided into four groups through unsupervised clustering. (B) We established a prognostic model using a multi-level attention graph neural algorithm. The model can distinguish patients into high-risk and low-risk groups with significant differences in DFS. (C) We identified key genes using the LASSO regression model and validated their roles in the development of prostate cancer through experiments. DFS: Disease-free survival; expr: Expression; FC: Fold change; LASSO: Least absolute shrinkage and selection operator; lncRNA: Long non-coding ribonucleic acid; LP: Linear projection; TCGA: The Cancer Genome Atlas; TOM: Topological overlap matrix; WGCNA: Weighted gene co-expression network analysis.

## ARTICLE INFO

Managing Editor: Peng Lyu

*Keywords:*
Prostate cancer
Cuproptosis

## ABSTRACT

*Background:* Long non-coding ribonucleic acids (lncRNAs) regulate messenger RNA (mRNA) expression and influence cancer development and progression. Cuproptosis, a newly discovered form of cell death, plays an important role in cancer. Nonetheless, additional research investigating the association between cuproptosis-related lncRNAs and prostate cancer (PCa) prognosis is required.

☆ Given his role as Guest Editor of the special issue on "Influence of tumor microenvironment on drug resistance of tumor", Prof. Hai Huang had no involvement in the peer-review of this article and has no access to information regarding its peer-review. Full responsibility for the editorial process for this article was delegated to Managing Editor, Peng Lyu.

* Corresponding author: Guangdong Provincial Key Laboratory of Malignant Tumor Epigenetics and Gene Regulation, Sun Yat-sen Memorial Hospital, Sun Yat-sen University, Guangzhou, Guangdong 510120, China.
*E-mail address:* huangh9@mail.sysu.edu.cn (H. Huang).

[1] Haitao Zhong, Yiming Lai, Wenhao Ouyang, and Yunfang Yu contributed equally to this work.

https://doi.org/10.1016/j.cpt.2024.03.004
Received 21 December 2023; Received in revised form 17 March 2024; Accepted 26 March 2024

Deep learning
lncRNAs

*Methods:* Sequencing data and copy number variant data were obtained from 492 patients with PCa from The Cancer Genome Atlas (TCGA) Program. Prognostic models of PCa based on cuproptosis-related lncRNAs were constructed using a multi-level attention graph neural network (MLA-GNN) deep learning algorithm. Immune escape scoring was performed using Tumor Immune Dysfunction and Exclusion. Cellular experiments were conducted to explore the correlation between key lncRNAs and cuproptosis.
*Results:* Data from 492 patients with PCa were randomized into two groups at a 1:1 ratio. Prognostic modeling was successfully established using MLA-GNN. Survival analysis suggested that patients could be divided into high- and low-risk groups according to model scores and that there was a significant difference in disease-free survival (DFS) ($P < 0.01$). The area under the receiver operating characteristic (ROC) curve (AUC) indicated a strong predictive performance for the model, with AUCs of 0.913, 0.847, and 0.863 for the training group and 0.815, 0.907, and 0.866 for the test group at 12, 36, and 60 months, respectively. The immune escape score and immune microenvironment analysis suggested that the high-risk group corresponded to a stronger immune escape and a poorer immune microenvironment ($P < 0.05$). Cellular experiments revealed that the expression of all six key lncRNAs was upregulated in the presence of copper ion carriers ($P < 0.05$).
*Conclusions:* This study identified cuproptosis-related lncRNAs that were strongly associated with PCa prognosis. Key lncRNAs could affect copper metabolism and may serve as new therapeutic targets.

## Introduction

Prostate cancer (PCa) has emerged as the predominant malignancy affecting the male urinary system and has recently been recognized as the second most common cause of cancer-related mortality among men.[1] Advances in PCa treatment through surgery and radiation have led to favorable prognosis among patients with PCa. Nevertheless, the tumor, node, metastasis (TNM) stages, and immunohistochemical subtypes of PCa, being cancer specific to men, may have completely different prognoses. Thus, novel prognostic factors and therapeutic targets for PCa must be identified to guide clinical practice.

Cuproptosis, a form of copper-induced cell death, is closely associated with mitochondrial respiration. Recently, cuproptosis has been found to be closely associated with cancer development and progression.[2] The activation of cuproptosis in cancer cells is a new strategy in the treatment of cancer, particularly for cancers that do not respond to conventional therapies.[3] Current studies have shown that elesclomol can be used to treat copper overload in cells.[4,5] While limited studies have investigated cuproptosis and PCa, the relationship between cuproptosis and the prognosis of patients with PCa remains uncertain.[6,7] Hence, it is crucial to identify biomarkers related to cuproptosis in patients with PCa. This endeavor aims not only to elucidate the precise mechanism underlying cuproptosis but also to forecast patient prognoses.

Long non-coding ribonucleic acids (lncRNAs) are a subset of RNA transcripts >200 nucleotides in length that play a vital role in regulating messenger RNA (mRNA) expression and determining cancer development, occurrence, metastasis, and prognosis.[8,9] No study has yet investigated cuproptosis-related lncRNAs in PCa.

Therefore, the present study aimed (1) to identify cuproptosis-related lncRNAs in PCa, which could not only provide insights into cuproptosis in PCa but also predict prognosis, (2) to investigate the relationship between cuproptosis-related lncRNAs and immune microenvironment in PCa, and (3) to verify through cellular experiments whether lncRNAs are indeed regulated by the cuproptosis mechanism.

## Methods

### *Data source*

RNA sequencing (RNA-seq) expression profiles of 492 patients with PCa were obtained from The Cancer Genome Atlas (TCGA) Program, and their clinical data were acquired from cBioPortal (https://www.cbioportal.org/). The clinical endpoint was disease-free survival (DFS). A total of 19 cuproptosis-related genes were obtained from GeneCards (https://www.genecards.org/), and data on copy number variation (CNV) were acquired using the University of California, Santa Cruz (UCSC) Xena platform (https://xena.ucsc.edu/).

### *Exploration of cuproptosis-related long non-coding ribonucleic acids*

The correlation between the 19 cuproptosis-related lncRNAs was determined using Search Tool for the Retrieval of Interacting Genes/Proteins (STRING) (https://cn.string-db.org/). Furthermore, a Pearson correlation analysis was conducted using the "limma" package to identify cuproptosis-related lncRNAs, with correlation coefficients >0.5 and $P$ values < 0.001 being considered statistically significant.

### *Association between disease-free survival and cuproptosis-related long non-coding ribonucleic acids*

Unsupervised clustering was performed using "ConsensusClusterPlus" to distinguish patients with different expression levels of cuproptosis-related lncRNAs. Survival analysis of clusters was also conducted to examine the correlation between DFS and cuproptosis-related lncRNAs.

### *Establishment of the risk model*

A model was constructed using a multi-level attention graph neural network (MLA-GNN). Weighted gene co-expression network analysis (WGCNA) was first performed to determine the strength of the co-expression relationship between each gene; from this, the edge matrix $E(K \times K)$ was obtained. The feature matrix $V(K \times 1)$ corresponded to a graph with $K$ nodes, in which each node represented the expression level of a gene. The edge matrix $E$ and feature matrix $V$ were inputted into the advanced graph convolutional layer graph attention (GAT) to construct multi-level graph features. The GAT outputted each point feature as a weighted combination of its neighboring nodes and the node itself and performed a self-attention mechanism to compute the attention coefficients of the node and its neighbors. The attention coefficients were normalized using the softmax function. Linear projection was conducted through the fully connected layer to generate high-level graph features with reduced node dimensions. Subsequently, the features were vectorized to generate three same-dimensional feature vectors, which were concatenated to produce the fusion feature $F$.

$$F = \begin{bmatrix} F1 \\ F2 \\ F3 \end{bmatrix} = \begin{bmatrix} G1 \\ G'2 \\ G'3 \end{bmatrix} = \begin{bmatrix} G1 & \\ G2 & \cdot T2 \\ G3 & \cdot T3 \end{bmatrix}$$

The fusion feature $F$ was encoded by the sequential fully connected layer. Disease survival prediction was performed in the prediction module, with output "$y$" denoting the risk ratio. The Cox loss was calculated as follows:

$$F_{Cox} = -\sum\left(y_p - log_{y_q \geq y_p} \sum exp\left(y_q\right)\right)$$

The relationship between each prognostically relevant lncRNA and DFS in patients was explored. The deep learning algorithm calculated the risk score for each sample and categorized the patients into high- and low-risk groups according to the optimal threshold. The performance of the model was evaluated using the area under the receiver operating characteristic (ROC) curve (AUC).

*Function enrichment and tumor immune environment analysis*

The different expression of genes was assessed between high- and low-risk patients using the "limma" package, with |logfold change [FC] $\geq$ 0.5| being considered statistically significant. Gene Ontology (GO) analysis was conducted to detect patient enrichment in terms of biological processes (BPs), cellular components (CCs), and molecular functions (MFs). The activity of pathways was calculated via single-sample gene set enrichment analysis (ssGSEA) using the R package "gsva," and the result of gene set variation analysis (GSVA) was visualized using the R package "ggplot2."

The immune score of each patient was calculated using the R package "estimate," and the immune function score of each patient was calculated via ssGSEA. Each patient's immune escape score was obtained using Tumor Immune Dysfunction and Exclusion (TIDE, http://tide.dfci.harvard.edu/login/). The Tumor Mutational Burden (TMB) files were sorted out using "Reshape2" of the R package to integrate the DFS and analyze the impact of TMB on the prognosis.

*Acquisition of key long non-coding ribonucleic acids*

Least absolute shrinkage and selection operator (LASSO) regression was employed for predictor selection, and a correlation analysis was conducted to investigate the relationship between each crucial lncRNA and cuproptosis genes. A nomogram containing independent prognostic factors for PCa was constructed using the R package "nomogramEx," and hazard ratios (HRs) were calculated for lncRNAs using the "survival" package.

*Cell culture*

PC-3M-IE8 cells were cultured in Roswell Park Memorial Institute-1640 medium, whereas C4-2 cells were cultured in Dulbecco's modified Eagle's medium. Both culture media were supplemented with 100 U/mL penicillin and streptomycin, as well as 10% fetal bovine serum, and were maintained at 37 °C in a humidified atmosphere containing 5% carbon dioxide.

*Validation of key long non-coding ribonucleic acids*

Elesclomol, a copper ionophore, was acquired from Selleck Chemicals (Shanghai, China). Copper chloride was obtained from Sangon Corporation (Shanghai, China). The expression of lncRNAs was observed by adding elesclomol and copper chloride to the culture medium, with only elesclomol being added or neither.

An *in vitro* synthesized double-stranded DNA segment with cohesive termini compatible with BamHI and EcoRI enzymes and a hairpin structure 5′-CCATTCTCCTTGAAAGGACTTTTCAAGAGAAAGTCCTTTCAAGGA-GAATGG-3′ was inserted into polymerase chain reaction generating complementary-loop ligation variants (pGC-LV) vectors, followed by transfection into *Escherichia coli* DH5α for propagation. After amplification and selection, Invitrogen Life Technologies (Guangzhou, China) sequenced the positive clones, leading to plasmid extraction and recombination into the AC106820.5-short hairpin RNA (shRNA) lentiviral vector. Transfection of this vector into the PCa cell lines PC-3M-IE8 and C4-2 established the knockdown group (shAC106820.5), whereas cells harboring the control sequences composed the mock group (shNC).

*Statistical analysis*

In this study, deep learning modeling was performed using the supercomputing platform at Sun Yat-sen University. The related prognosis and immune microenvironment were analyzed using R software version 4.2.2 (R Foundation for Statistical Computing, Vienna, Austria). Experiment-related statistical plots were constructed using GraphPad Prism 8 software (GraphPad Software Inc., San Diego, CA, USA). Statistical significance was set at a $P$ value of $<0.05$.

## Results

A total of 492 patients with PCa with accompanying clinical data were enrolled in this study and were randomly divided into the training and validation groups at a 1:1 ratio. Supplementary Table 1 summarizes the baseline information.

*Acquisition and survival correlation of cuproptosis-related long non-coding ribonucleic acids*

First, the CNV locations of 19 copper death genes were counted on the chromosomes [Figure 1A]. CNV analysis indicated that most genes had copy number loss and that *ATP7B* and *GCSH* had higher mutation rates [Figure 1B].

Subsequently, the expression of 19 copper death-related genes was mutually promoted in both normal and PCa tissues, and this feature was more evident in tumor tissues [Figure 1C]. Protein interaction network analysis revealed interrelationships among the 19 cuproptosis-related genes [Figure 1D]. Through co-expression analysis, 231 cuproptosis-related lncRNAs were obtained, with Pearson correlation coefficient $>0.5$ and $P < 0.001$ as the criteria [Figure 2A]. Unsupervised clustering was performed according to the expression differences of these lncRNAs, and the patients were successfully divided into four categories [Figure 2B and Supplementary Figure 1A–C]. Survival analysis suggested differences in DFS among the four groups [Figure 2C]. Thus, the expression of these cuproptosis-related lncRNAs could affect DFS in patients.

*Model establishment and prognostic analysis*

We built a PCa prognostic model based on cuproptosis-related lncRNAs using the MLA-GNN deep learning algorithm. In the training group, the patients were categorized into high- and low-risk groups according to the optimal cutoff value of their risk scores. The two groups exhibited a significant difference in DFS ($P < 0.001$) [Figure 2D]. Additionally, the AUCs at 12, 36, and 60 months were 0.913, 0.874, and 0.863, respectively, suggesting the good predictive efficacy of the model [Figure 2F]. This result was validated in the validation group [Figure 2E and G].

Next, 12 cuproptosis-related lncRNAs with prognostic significance were screened via a LASSO regression analysis [Figure 3A and B]. Overall, six cuproptosis-related lncRNAs with prognostic significance were identified through a multivariate Cox regression analysis—namely, AC017100.1, AP001893.1, AC106820.5, AC009065.4, AC124854.1, and AC008966.1. These six lncRNAs showed a strong positive or negative correlation with cuproptosis-related genes [Figure 3C]. Survival analysis revealed that all six lncRNAs were associated with DFS; additionally, their beneficial or detrimental effects on survival were consistent with whether they were positively or negatively correlated with the expression of cuproptosis-related genes [Figure 3D–I].

Both univariate and multivariate independent prognostic analyses confirmed that the risk score of the model was a stable predictor ($P < 0.05$) [Figure 4A and B]. Furthermore, a discernible difference in DFS was noted between high- and low-risk patients, especially when considering the different Gleason scores [Figure 4C and D]. We obtained the genes in the differential risk table by differentially expressing the genes in the high- and low-risk groups and then determined the pathway differences between these two groups using these genes [Supplementary Figure 1D and E].

Based on the results of the multivariate Cox analysis, we constructed a nomogram using the Gleason and risk scores [Figure 4E]. The calibration curves at 5 and 8 years indicated a high degree of fitness between the predicted DFS from the nomogram score and the actual DFS [Figure 4F].

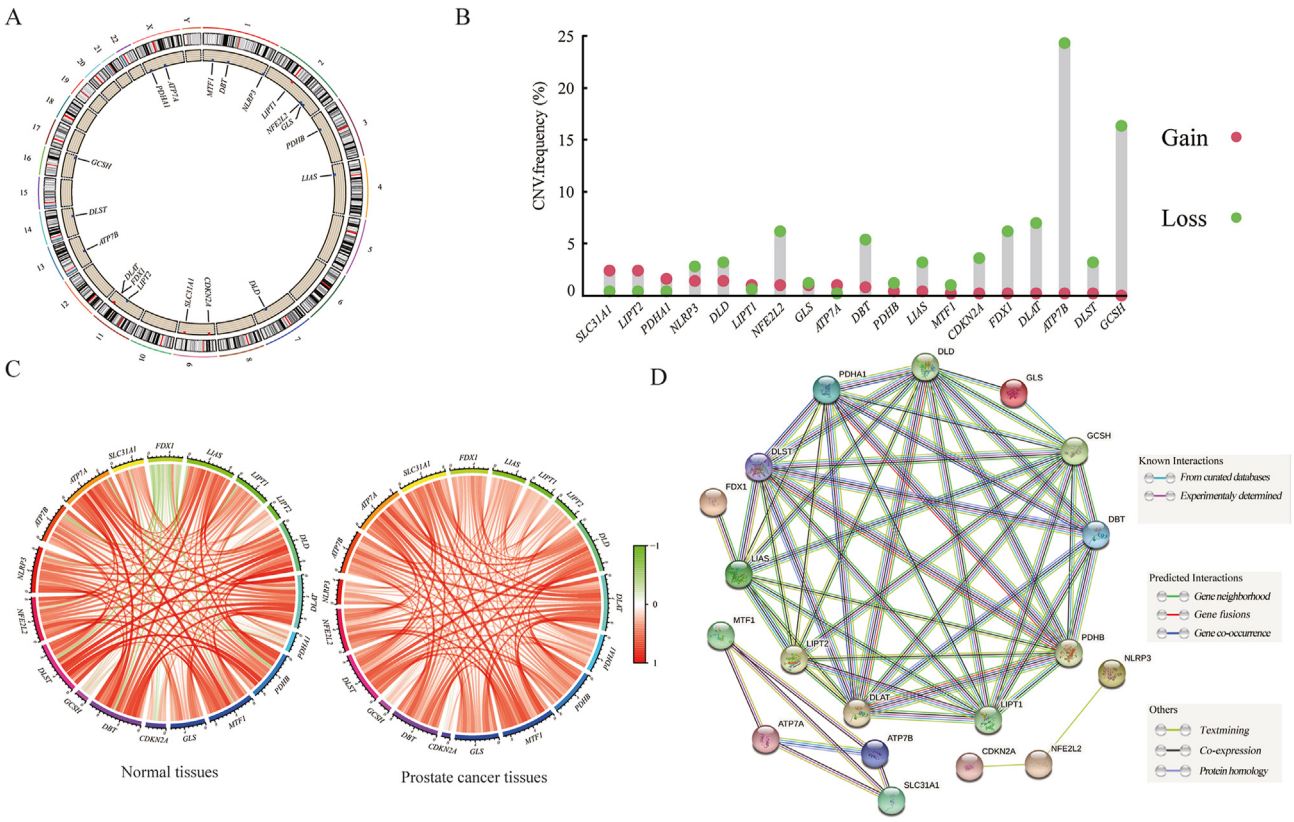


**Figure 1.** Distribution and expression of cuproptosis-related genes. (A) Circle diagram of the distribution of cuproptosis-related genes on chromosomes. (B) Copy number variation (CNV) of cuproptosis-related genes. (C) Expression correlation of 19 cuproptosis-related genes. (D) Protein interaction of 19 cuproptosis-related genes. CNV: Copy number variation.

The AUC was further enhanced, suggesting that the incorporation of clinical features could optimize the model and better predict the DFS [Figure 4G]. These findings imply a significant improvement in prognostic accuracy with the integration of clinical characteristics.

*Immune infiltration in different risk groups*

Analysis of patients' immune escape scores in different risk groups revealed that patients in the high-risk group were more prone to immune escape [Figure 5A]. Further analysis of patients' immune microenvironment in both groups showed that the expression levels of three immune checkpoints (namely, cytotoxic T-lymphocyte associated protein 4 [*CTLA-4*], programmed death-ligand 1 [*PD-L1*], and lymphocyte-activation gene 3 [*LAG3*]) were increased in the high-risk group [Figure 5B–D]. Differential analysis indicated that the expression levels of immune cells were lower in the high-risk group [Figure 5E]. These results suggest that the immune microenvironment of patients in the high-risk group is more suppressed, and it is easier for them to escape killing by the immune system owing to the occurrence of copper death resistance.

Verification of association between cuproptosis-related long noncoding ribonucleic acids and cuproptosis

Primers were custom-synthesized by Sangon Biotech (Shanghai, China), and their sequences are listed in Table 1. Our assessment aimed to determine whether copper affected the expression of these six lncRNAs. Copper was transported into the cells by the copper ionophore elesclomol. Copper chloride (2 mmol/L) or elesclomol (20 mmol/L) or both were used in the PCa cell lines for 24 h, and the expression of the six lncRNAs in the two PCa cell lines was observed using quantitative reverse-transcription polymerase chain reaction (qRT-PCR). In the presence of elesclomol, the six lncRNAs were significantly upregulated when exogenous copper ions were introduced into the PCa cell lines exposed to copper [Figure 6], suggesting that these lncRNAs play an important role in copper poisoning in PCa.

The HRs for the six lncRNAs and model scores were obtained using Cox regression analysis, which indicated that AC106820.5 had the highest HR [Figure 7A]. Therefore, we selected this lncRNA as the key gene for the cellular experiments. The expression of AC106820.5 was stably reduced by shRNA [Figure 7B]. Transwell experiments showed that the proliferation and migration abilities of PCa cells were significantly inhibited after the knockdown of AC106820.5 expression [Figure 7C and D]. The plate cloning assay revealed that the proliferation of PCa cells was inhibited by the knockdown of AC106820.5 [Figure 7E], whereas the Cell Counting Kit-8 (CCK8) assay showed that the knockdown of AC106820.5 reduced the proliferation of PCa cells [Figure 7F]. Combined with the qPCR results, these findings suggest that AC106820.5 may enhance cellular adaptation to copper death in PCa but may promote PCa progression through cell proliferation, migration, and invasion.

## Discussion

In this study, we successfully developed a PCa prognostic model based on cuproptosis-related lncRNAs using a deep-learning algorithm. Patients were divided into high- and low-risk groups according to risk scores, and the ROC curve analysis suggested that our model had excellent predictive efficacy. Further, through LASSO regression and multifactorial Cox algorithm, we identified six hub lncRNAs that were strongly correlated with DFS among patients. Additionally, patients in the high-risk group had elevated immune escape scores and exhibited heightened expression of immune checkpoints, potentially influencing the less favorable prognosis within this group. Finally, *in vitro* cellular experiments revealed a strong correlation between these six lncRNAs and cuproptosis gene expression. Further experiments targeting AC106820.5, which had the highest risk ratio, showed that knocking it down inhibited the proliferation, invasion, and migration of PCa cells, suggesting that these genes play an essential role in the initiation of cuproptosis in cancer cells.

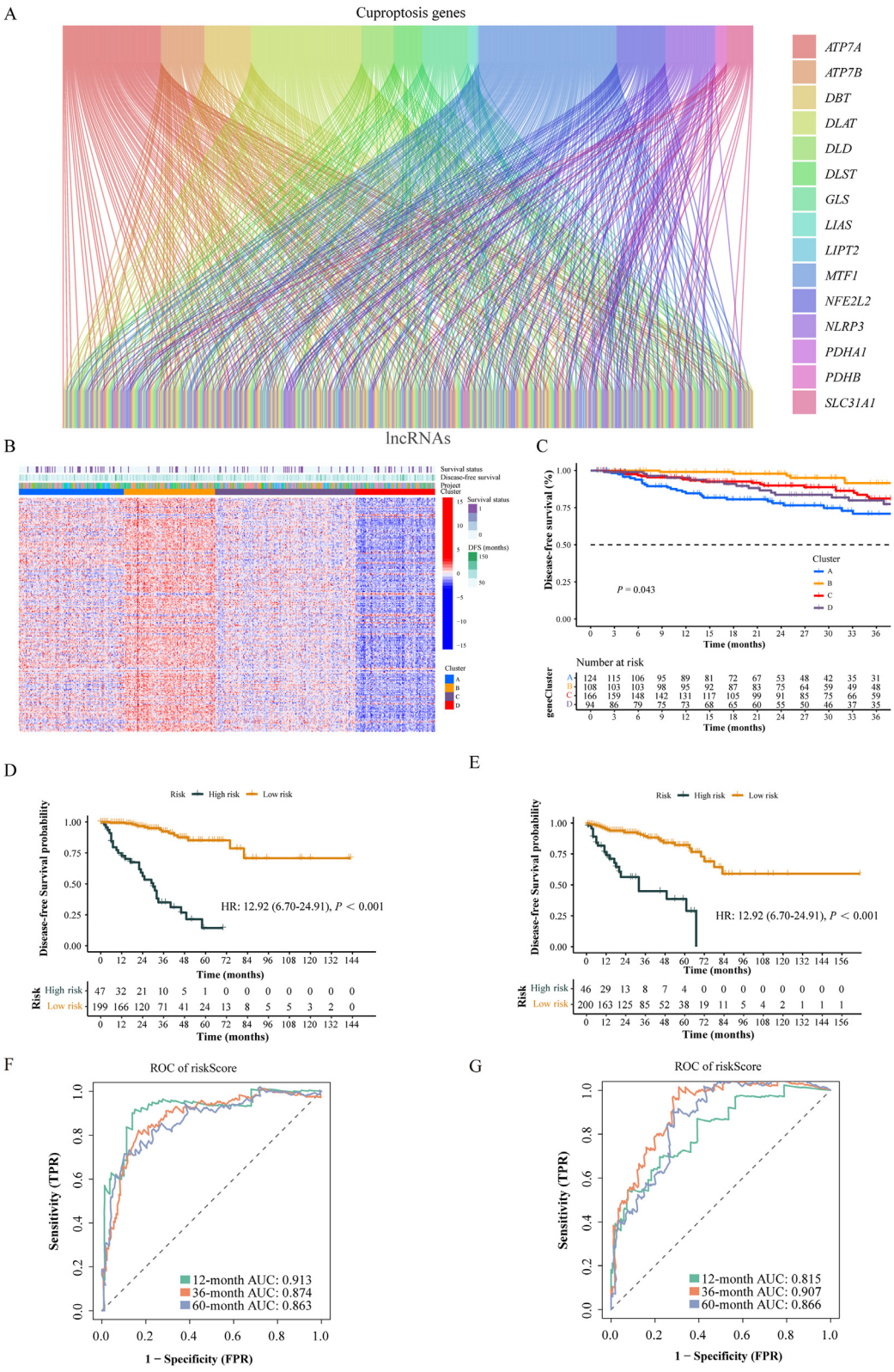


**Figure 2.** Unsupervised clustering and model establishment of cuproptosis-related lncRNAs. (A) Co-expression of cuproptosis-related lncRNAs and cuproptosis-related genes. (B) Heatmap of differentially expressed cuproptosis-related lncRNAs among the four cluster subgroups. Each row of the heatmap represents a cuproptosis-related lncRNA, whereas each column represents a patient. The color signifies the level of expression: the color near to red indicates high expression, whereas the color near to blue indicates low expression. (C) Kaplan–Meier curve of disease-free survival (DFS) in patients in the four subgroups. (D) Kaplan–Meier curve for DFS in patients in the training group. (E) Kaplan–Meier curve for DFS in patients in the validating group. (F) The receiver operating characteristic (ROC) analysis proved the prognostic performance of the model in the training group. (G) The ROC analysis proved the prognostic performance of the model in the validating group. AUC: Area under the receiver operating characteristic curve; DFS: Disease-free survival; FPR: False positive rate; HR: Hazard ratio; lncRNA: Long non-coding ribonucleic acid; ROC: Receiver operating characteristic; TPR: Ture positive rate.

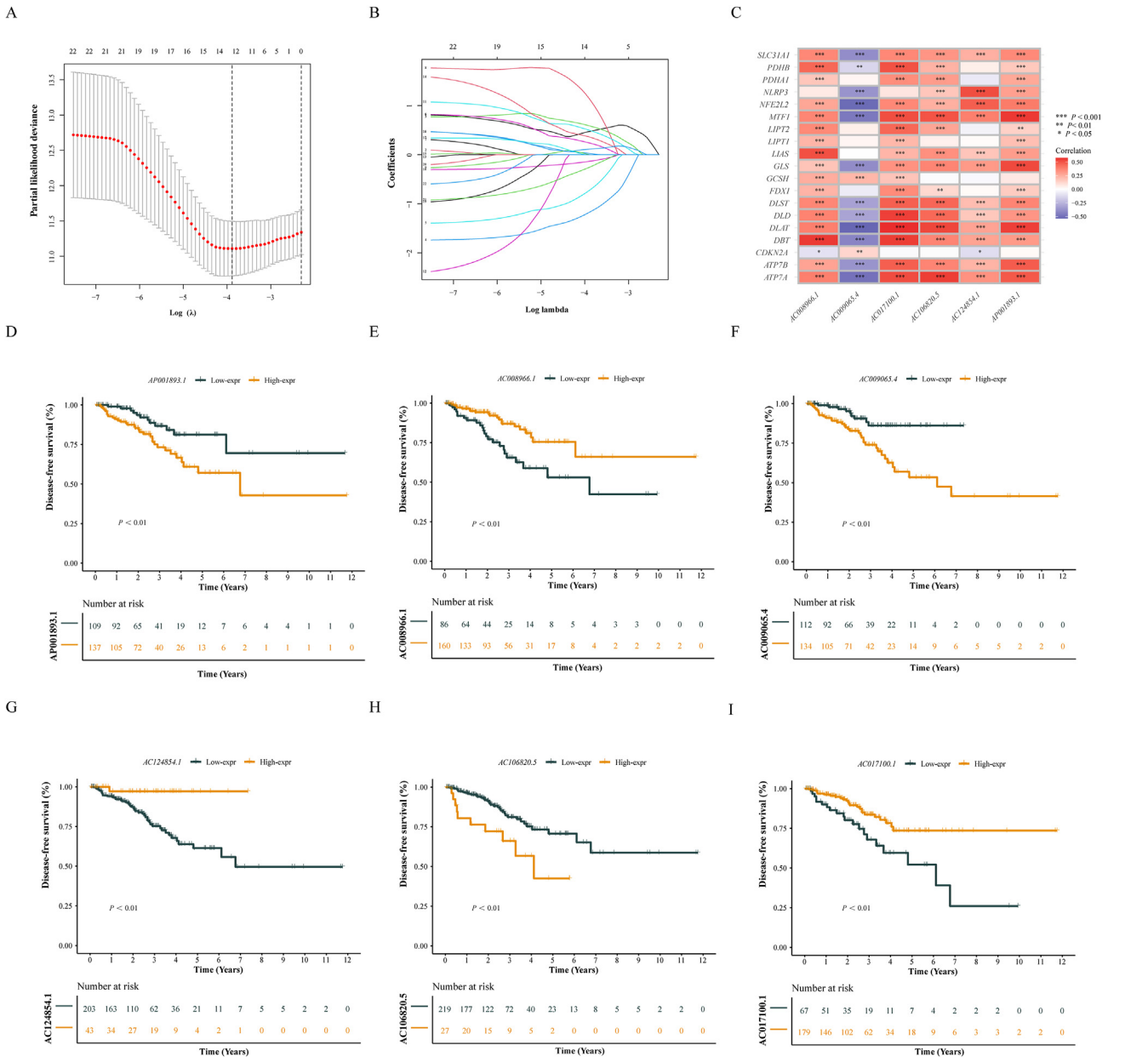


**Figure 3.** Screening of key lncRNAs and their survival relevance. (A) Confidence intervals for each lambda are shown. Vertical dots are drawn at ideal values using the minimum criteria. (B) Partial likelihood deviations for various counts. The coefficient of the independent variable lambda is shown on the vertical axis, whereas its log value is represented on the horizontal axis. (C) Heatmap of the correlation between cuproptosis-related genes and lncRNAs. Each row in the heat map represents a cuproptosis-related gene, whereas each column represents cuproptosis-related lncRNAs. The color signifies the correlation: the color near blue indicates a negative correlation, whereas the color near red indicates a positive correlation (*$P < 0.05$, **$P < 0.01$, ***$P < 0.001$; ns, not significant). (D–I) Kaplan–Meier curve for the six key lncRNAs associated with disease-free survival. expr: Expression; lncRNA: Long non-coding ribonucleic acid; ns: Not significant.

Copper toxicity is a cell death process associated with mitochondrial respiration.[10,11] Copper, a key factor in the copper death pathway, plays two main roles. On the one hand, copper acts as a cofactor for various enzymes, oxygen metabolism, and oxygen radical detoxification.[12,13] On the other hand, copper accumulation causes a series of metabolic dysfunctions in cells, ultimately leading to cell death.[14] Recently, numerous studies have identified copper ions as significant contributors to tumorigenesis. In breast, thyroid, gastric, lung, and other cancers, serum copper ions were reported to be higher in patients with tumors than in normal people[15–18]; it was also found that the higher the serum copper ions, the worse the prognosis of patients with lung cancer. Serum copper and iron ion levels were also significantly higher in PCa than in prostatic hyperplasia.[19] This suggests that copper ions play a key role in cancer progression. Our study showed that patients with PCa had a loss mutation in the cuproptosis gene relative to healthy individuals or patients with prostate hyperplasia. This loss mutation may lead to a reduction in the number of vectors that mediate the entry of copper ions into the cells, thereby reducing copper-associated programmed cell death. This may also contribute to the elevated serum copper ion concentrations in patients with cancer.

In recent years, several studies have attempted to utilize ncRNAs to predict the survival of patients with cancer. Li et al.[20] revealed that lncRNA AP004608.1 could serve as a potential prognostic biomarker for PCa, offering promise as a therapeutic target. In addition, lncRNA KCNQ1OT1 promoted the invasion and migration of PCa via PTP4A3 upregulation, suggesting that lncRNAs are actively involved in PCa genome regulation.[21] Our study verified that copper death-related lncRNAs could categorize patients with PCa into four molecular

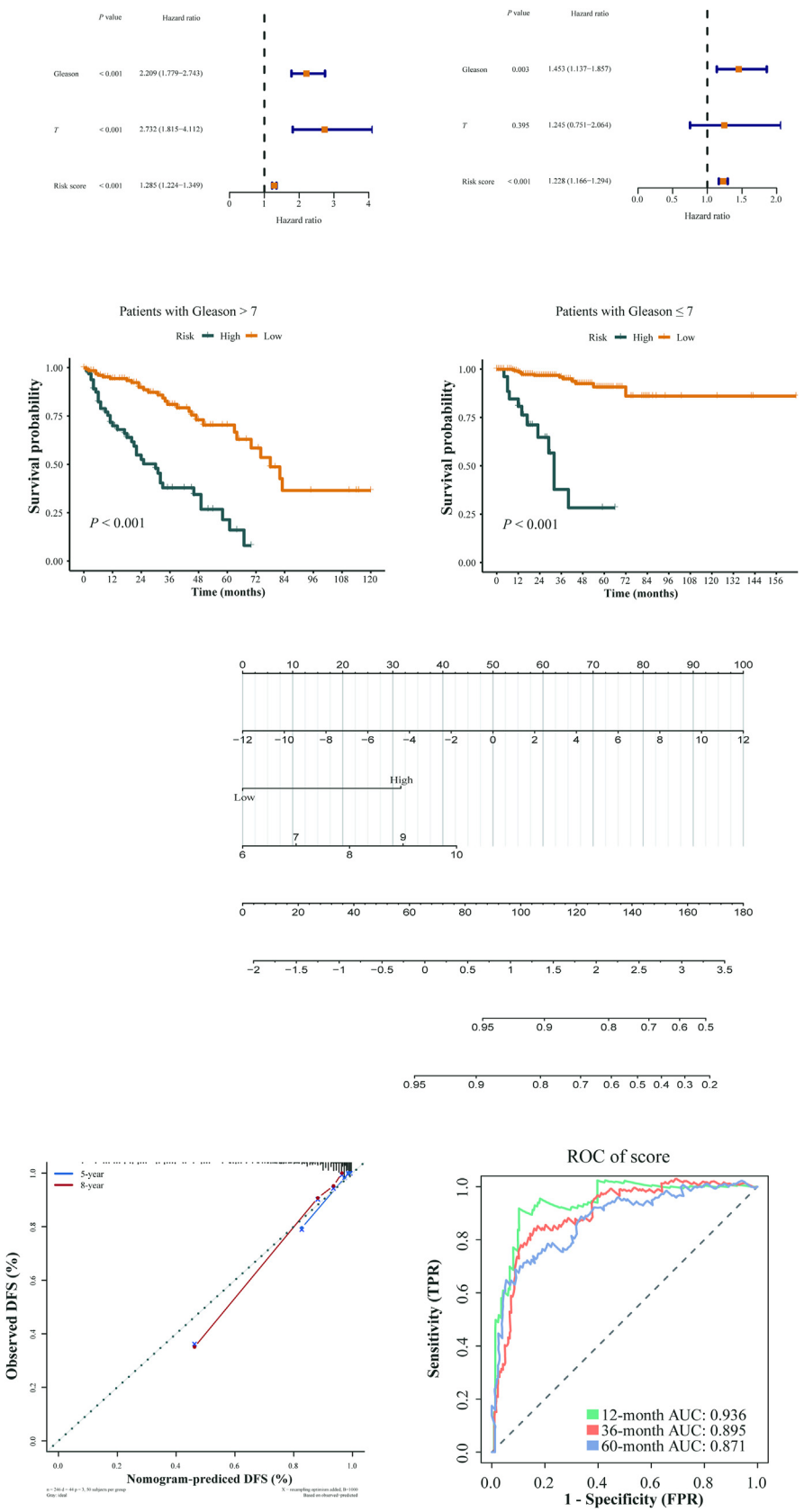


**Figure 4.** Independent prognostic analysis in all patients. (A) Univariate independent prognosis of clinical characteristics and risk scores. (B) Multivariate independent prognosis of clinical characteristics and risk scores. (C) Kaplan–Meier curve for disease-free survival (DFS) in patients with a Gleason score of >7. (D) Kaplan–Meier curve for DFS in patients with a Gleason score of ≤7. (E) Gleason risk scores. (F) 5- and 8-year corrected curves of the nomogram. (G) The ROC analysis demonstrates the prognostic performance of the nomogram. AUC: Area under the receiver operating characteristic curve; DFS: Disease-free survival; FPR: False positive rate; ROC: Receiver operating characteristic; TPR: Ture positive rate.

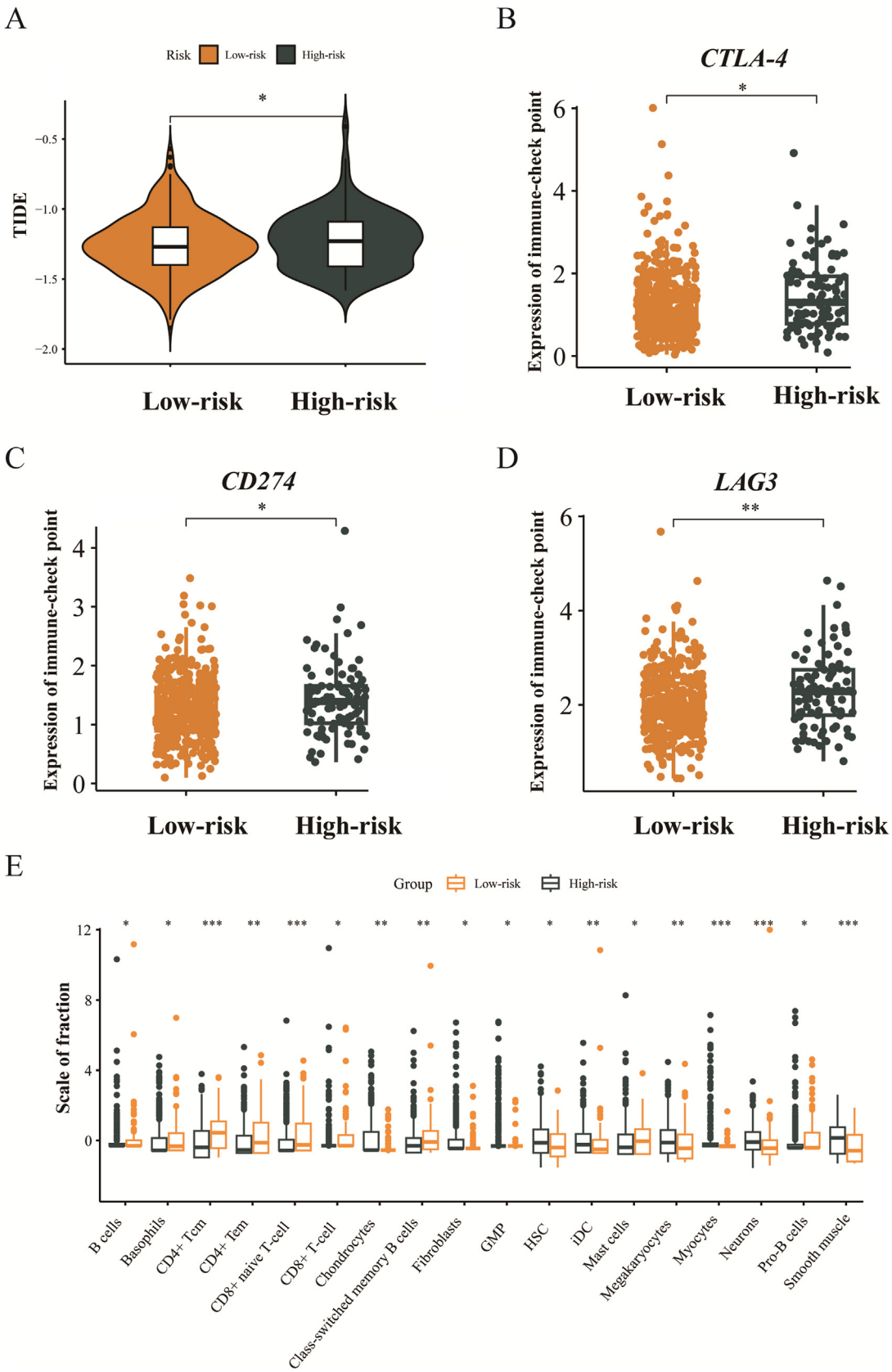


**Figure 5.** Differences in the immune microenvironment of patients in the two risk groups. (A) Tumor Immune Dysfunction and Exclusion (TIDE) scores in the two risk groups. (B–D) Immune checkpoint expression levels in the two groups. (E) Immune cell protein expression levels in both groups (ns, $P \geq 0.05$; *$P < 0.05$, **$P < 0.01$, ***$P < 0.001$). *CD274*: Cluster of differentiation 274; *CTLA-4*: Cytotoxic T-lymphocyte associated protein 4; GMP: Granulocyte-Macrophage Progenitors; HSC: Hematopoietic Stem Cells; iDC: Immature Dendritic Cells; *LAG3*: Lymphocyte-activation gene 3; ns: Not significant; Tcm: Central Memory T-Cell; Tem: Effector Memory T-Cell; TIDE: Tumor Immune Dysfunction and Exclusion.

**Table 1**
Primers for six cuproptosis-related lncRNAs.

| LncRNA | Primer sequence |
|---|---|
| AC017100.1 | Forward: 5′-AACGGACGGGTGTCTTCATC-3′<br>Reverse 5′-AAAGAAACACCTGCGCACAC-3′ |
| AP001893.1 | Forward 5′-CCTCTGGTTCTTACTCAACGCA-3′<br>Reverse 5′-GCGTACACCAGACACGCATA-3′ |
| AC106820.5 | Forward 5′-CATGACTTCCTGGCCTGATGG-3′<br>Reverse 5′-GTGTGACATGACTTCCCTCCC-3′ |
| AC009065.4 | Forward 5′-AAGAGCGACGAGCTTGAGAG-3′<br>Reverse 5′-TACAGTGAGACTCCATCTCGG-3′ |
| AC124854.1 | Forward 5′-GCGTTTAAGTGTTTGGGCGA-3′<br>Reverse 5′-GTTGAAGTAGAAGCAGCTGCAAG-3′ |
| AC008966.1 | Forward 5′-AGTGAACGAGGGTGAGGACT-3′<br>Reverse 5′-CCTTCTTAGTGGCCAGTCACC-3′ |

lncRNA: Long non-coding ribonucleic acid.

subtypes and demonstrated a significant difference in patient survival between these four subtypes. This suggests that cuproptosis-associated lncRNAs affect the survival of patients with PCa by regulating the expression of cuproptosis genes.

Intersections between disciplines often collide, producing outstanding results. Recently, the use of machine learning in the field of medicine has become widespread, yielding promising outcomes.[22] Human genetic data are large and complex, and the information that they contain has great potential for disease prevention and treatment.[23–26] However, it is difficult to process and analyze a large amount of information. Fortunately, computers can be used to address this problem, and machine learning allows computers to extract features from data for learning and making predictions. As the amount of data increases, so does the amount of information that can be analyzed, and the model can become more stable and accurate. We successfully constructed a PCa prognostic model with copper death-related lncRNAs using the MLA-GNN deep learning algorithm. The Kaplan–Meier (K–M) survival curves suggested that patients could be classified into two categories according to the model scores, and there was a significant DFS gap. The ROC curve showed that the predictive efficacy of the model was good. The independent prognostic analysis also concluded that the model's score was an independent prognostic factor, along with recognized clinical prognostic characteristics such as the Gleason score.

Cancer progression is typically accompanied by changes in immune microenvironment.[27–29] We analyzed differences in the immune microenvironment based on gene expression between the two groups of patients. Patients in the high-risk group had higher immune escape scores. This result is consistent with that of a previous study on renal and lung cancers,[30] suggesting that copper death-related lncRNAs influence the immune escape of cells by regulating the expression of copper death genes. In contrast, the high-risk group exhibited elevated levels of CTLA-4, LAG3, and cluster of differentiation 274 (CD274), signifying a less favorable immune microenvironment. These factors may contribute to an unfavorable prognosis.

In a previous study, AC017100.1 was reported to be included in a competing endogenous RNA (ceRNA) signature for PCa prognosis and might be involved in the 5-methylcytosine (m5C) methylation of RNA.[31] Jiang et al. reported that AC124854.1 had an impact on renal cell carcinoma prognosis. In fact, when considered alongside our discoveries,

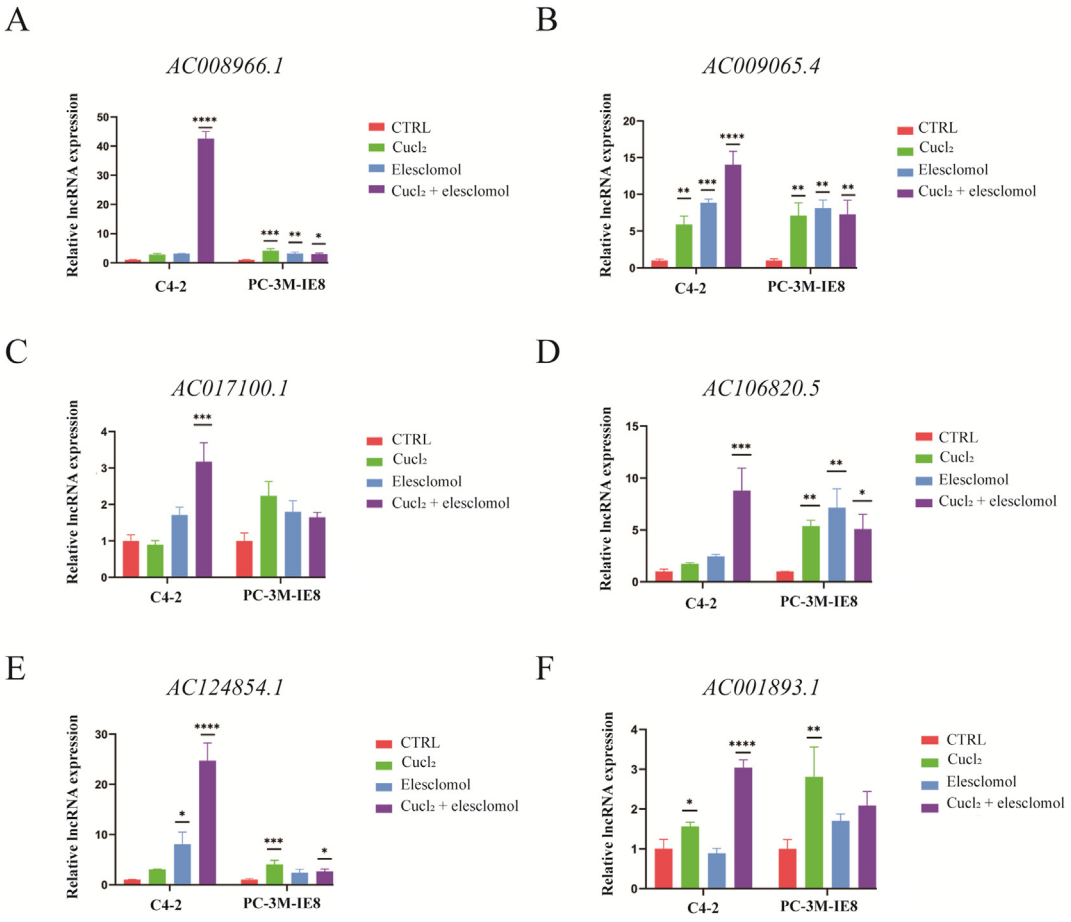


**Figure 6.** Relationship between lncRNAs and copper ions. (A–F) Differences in the expression levels of lncRNAs in two cell lines, C4-2 and PC-3M-IE8, with or without the addition of copper ion carriers (*$P < 0.05$, **$P < 0.01$, ***$P < 0.001$). CTRL: Control; lncRNA: Long non-coding ribonucleic acid.

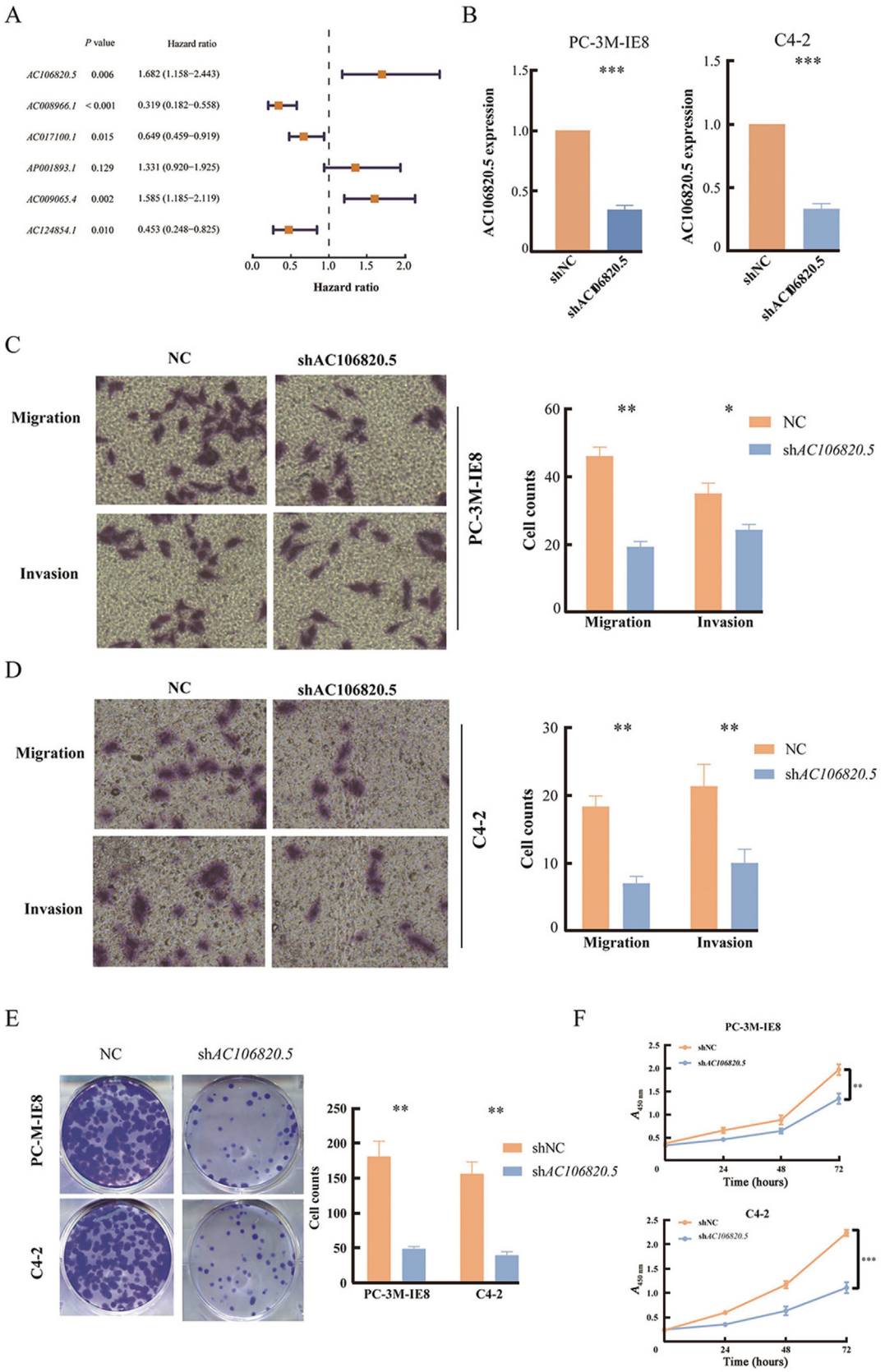


**Figure 7.** Validation of key lncRNAs. (A) Forest plot of hazard ratios for the six lncRNAs. (B) Knockdown inefficiencies for AC106820.5. (C) The invasive and migratory capacities of PC-3M-IE8 cells after AC106820.5 knockdown. The image magnification was 20 × . (D) The invasive and migratory capacities of C4-2 cells after AC106820.5 knockdown. The image magnification was 20 × . (E) Plate cloning experiments on PC-3M-IE8 and C4-2 cells before and after AC106820.5 knockdown. (F) CCK8 experiments on PC-3M-IE8 and C4-2 cells before and after AC106820.5 knockdown. C4-2: The human prostate cancer cell line; CCK8: Cell Counting Kit-8; lncRNA: Long non-coding ribonucleic acid; NC: Negative control; PC-3M-IE8: The human prostate cancer cell line; shNC: Short hairpin RNA negative control.

this implies that AC009065.4 may have a connection with both cuproptosis and ferroptosis, hinting at a potential interplay between the mechanisms mediated by cuproptosis and ferroptosis.[32–34] High concentrations of reactive oxygen species caused by copper induce mitochondrial dysfunction, which leads to accelerated cell death, and the hydroxyl radicals generated by the copper-based Fenton reaction can damage DNA after copper complexes are inserted into DNA.[35] In the present study, we identified six prognostic lncRNAs: AC017100.1, AP001893.1, AC106820.5, AC009065.4, AC124854.1, and AC008966.1. Using these lncRNAs, we predicted the prognosis of patients with PCa. We found that these lncRNAs were significantly upregulated after treating with $CuCl_2$ and elesclomol on PCa cells, suggesting that they were also upregulated. Considering the close relationship between cuproptosis and these lncRNAs, they may provide new insights into the treatment of PCa.

This study has some limitations. First, additional data to further refine the model were lacking. Second, experimental validation of all key lncRNAs, which was limited by experimental conditions, could not be performed. These shortcomings will be addressed in future studies.

In conclusion, we identified copper death-related lncRNAs that were associated with PCa prognosis. The high-risk group corresponded to stronger immune escape and poorer immune microenvironment. Key lncRNAs could influence copper metabolism and may be novel therapeutic targets.

## Authors contribution

Haitao Zhong and Wenhao Ouyang: formal analysis, writing – original draft; Yongxin Wu: data curation, methodology; Xinxin He, Lexiang Zeng, and Xueen Qiu: data curation; Peixian Chen, Lingfeng Li, Jie Zhou, and Tianlong Luo: project administration, resources; Yiming Lai: funding acquisition, writing – review & editing; Yunfang Yu: funding acquisition, conceptualization; Hai Huang: funding acquisition, supervision, writing – review & editing. All the authors have read and approved the final version of the manuscript.

## Ethics statement

All procedures involving human participants were conducted in accordance with the 1964 *Declaration of Helsinki* and its later amendments or comparable ethical standards.

## Declaration of generative AI and AI-assisted technologies in the writing process

The authors declare that generative artificial intelligence (AI) and AI assisted technologies were not used in the writing process or any other process during the preparation of this manuscript.

## Funding

This work was supported by grants from the National Natural Science Foundation of China (Nos. 82372912, 81802527, 81972471, 82073408, 81974395, and 82173036), National Key Research and Development Program of China (Nos. 2022YFC3602900 and 2022YFC3602904), Beijing Bethune Charitable Foundation (Nos. mnzl202001 and mnzl202026), Guangzhou Science and Technology Project (Nos. 202206010078 and 202201020574), Sun Yat-sen University Clinical Research 5010 Program (Nos. 2018007 and 2019005), Sun Yat-sen Clinical Research Cultivating Program (No. SYS-C-201801), Guangdong Medical Science and Technology Program (No. A2020558), Tencent Charity Foundation (No. 7670020025), Scientific Research Launch Project of Sun Yat-sen Memorial Hospital (No. YXQH202209), Guangdong Basic and Applied Basic Research Foundation (No. 2019A1515011437), International Science and Technology Cooperation Project Plan of Guangdong Province (No. 2021A0505030085), Guangzhou Science and Technology Key R&D Project (No. 202206010117), Beijing CSCO Clinical Oncology Research Foundation (No. Y-tongshu2021/ms-0162), Guangdong Provincial Clinical Research Center for Urological Diseases (No. 2020B1111170006), and Guangdong Science and Technology Department (No. 2020B1212060018), as well as open research funds from the Sixth Affiliated Hospital of Guangzhou Medical University, Qingyuan People's Hospital.

## Conflict of interest

The authors declare that they have no known competing financial interests or personal relationships that could have appeared to influence the work reported in this paper.

## Acknowledgments

None.

## Appendix A. Supplementary data

Supplementary data to this article can be found online at https://doi.org/10.1016/j.cpt.2024.03.004.

## Data availability statement

Data access for the article can be obtained by contacting the corresponding authors.

## References

1. Culp MB, Soerjomataram I, Efstathiou JA, Bray F, Jemal A. Recent global patterns in prostate cancer incidence and mortality rates. *Eur Urol*. 2020;77:38–52. https://doi.org/10.1016/j.eururo.2019.08.005.
2. Xie J, Yang Y, Gao Y, He J. Cuproptosis: mechanisms and links with cancers. *Mol Cancer*. 2023;22:46. https://doi.org/10.1186/s12943-023-01732-y.
3. Tong X, Tang R, Xiao M, et al. Targeting cell death pathways for cancer therapy: recent developments in necroptosis, pyroptosis, ferroptosis, and cuproptosis research. *J Hematol Oncol*. 2022;15:174. https://doi.org/10.1186/s13045-022-01392-3.
4. Zheng P, Zhou C, Lu L, Liu B, Ding Y. Elesclomol: a copper ionophore targeting mitochondrial metabolism for cancer therapy. *J Exp Clin Cancer Res*. 2022;41:271. https://doi.org/10.1186/s13046-022-02485-0.
5. Gao W, Huang Z, Duan J, Nice EC, Lin J, Huang C. Elesclomol induces copper-dependent ferroptosis in colorectal cancer cells via degradation of ATP7A. *Mol Oncol*. 2021;15:3527–3544. https://doi.org/10.1002/1878-0261.13079.
6. Jin L, Mei Wangli, Liu X, et al. Identification of cuproptosis-related subtypes, the development of a prognosis model, and characterization of tumor microenvironment infiltration in prostate cancer. *Front Immunol*. 2022;13:974034. https://doi.org/10.3389/fimmu.2022.974034.
7. Cheng B, Tang C, Xie Junjia, et al. Cuproptosis illustrates tumor micro-environment features and predicts prostate cancer therapeutic sensitivity and prognosis. *Life Sci*. 2023;325:121659. https://doi.org/10.1016/j.lfs.2023.121659.
8. Lin W, Zhou Q, Wang CQ, et al. lncRNAs regulate metabolism in cancer. *Int J Biol Sci*. 2020;16:1194–1206. https://doi.org/10.7150/ijbs.40769.
9. Wang Q, Cheng B, Singh S, et al. A protein-encoding CCDC7 circular RNA inhibits the progression of prostate cancer by up-regulating FLRT3. *npj Precis Oncol*. 2024;8:11. https://doi.org/10.1038/s41698-024-00503-2.
10. Tang D, Chen X, Kroemer G. Cuproptosis: a copper-triggered modality of mitochondrial cell death. *Cell Res*. 2022;32:417–418. https://doi.org/10.1038/s41422-022-00653-7.
11. Xiong Z, Tong T, Xie Z, et al. Delivery of gefitinib loaded nanoparticles for effectively inhibiting prostate cancer progression. *Biomater Sci*. 2024;12:650–659. https://doi.org/10.1039/d3bm01735d.
12. Festa RA, Thiele DJ. Copper: an essential metal in biology. *Curr Biol*. 2011;21:R877–R883. https://doi.org/10.1016/j.cub.2011.09.040.
13. Robinson NJ, Winge DR. Copper metallochaperones. *Annu Rev Biochem*. 2010;79:537–562. https://doi.org/10.1146/annurev-biochem-030409-143539.
14. Cobine PA, Moore SA, Leary SC. Getting out what you put in: copper in mitochondria and its impacts on human disease. *Biochim Biophys Acta Mol Cell Res*. 2021;1868:118867. https://doi.org/10.1016/j.bbamcr.2020.118867.
15. Pavithra V, Sathisha TG, Kasturi K, Mallika DS, Amos SJ, Ragunatha S. Serum levels of metal ions in female patients with breast cancer. *J Clin Diagn Res*. 2015;9:BC25–Bc27. https://doi.org/10.7860/JCDR/2015/11627.5476.
16. Kosova F, Cetin B, Akinci M, et al. Serum copper levels in benign and malignant thyroid diseases. *Bratisl Lek Listy*. 2012;113:718–720. https://doi.org/10.4149/bll_2012_162.

17. Basu S, Singh MK, Singh TB, Bhartiya SK, Singh SP, Shukla VK. Heavy and trace metals in carcinoma of the gallbladder. *World J Surg*. 2013;37:2641–2646. https://doi.org/10.1007/s00268-013-2164-9.
18. Wang W, Wang X, Luo J, et al. Serum copper level and the copper-to-zinc ratio could be useful in the prediction of lung cancer and its prognosis: a case-control study in Northeast China. *Nutr Cancer*. 2021;73:1908–1915. https://doi.org/10.1080/01635581.2020.1817957.
19. Saleh SAK, Adly HM, Abdelkhaliq AA, Nassir AM. Serum levels of selenium, zinc, copper, manganese, and iron in prostate cancer patients. *Curr Urol*. 2020;14:44–49. https://doi.org/10.1159/000499261.
20. Wei L, Runze Z, Bo S, Jin X, Chen Y, Xu X. Prognostic significance of lncRNA AP004608.1 in prostate cancer. *Front Oncol*. 2022;12:1017635. https://doi.org/10.3389/fonc.2022.1017635.
21. Wang Y, Guo Y, Lu Y, Sun Y, Xu D. The effects of endosulfan on cell migration and invasion in prostate cancer cells via the KCNQ1OT1/miR-137-3p/PTP4A3 axis. *Sci Total Environ*. 2022;845:157252. https://doi.org/10.1016/j.scitotenv.2022.157252.
22. Rauschert S, Raubenheimer K, Melton PE, Huang RC. Machine learning and clinical epigenetics: a review of challenges for diagnosis and classification. *Clin Epigenet*. 2020;12:51. https://doi.org/10.1186/s13148-020-00842-4.
23. Rodenhiser D, Mann M. Epigenetics and human disease: Translating basic biology into clinical applications. *CMAJ (Can Med Assoc J)*. 2006;174:341–348. https://doi.org/10.1503/cmaj.050774.
24. Krittanawong C, Zhang H, Wang Z, Aydar M, Kitai T. Artificial intelligence in precision cardiovascular medicine. *J Am Coll Cardiol*. 2017;69:2657–2664. https://doi.org/10.1016/j.jacc.2017.03.571.
25. Suzuki T, Otsuka M, Seimiya T, Iwata T, Kishikawa T, Koike K. The biological role of metabolic reprogramming in pancreatic cancer. *MedComm*. 2020;1:302–310. https://doi.org/10.1002/mco2.37.
26. Yu Y, He Z, Ouyang J, et al. Magnetic resonance imaging radiomics predicts preoperative axillary lymph node metastasis to support surgical decisions and is associated with tumor microenvironment in invasive breast cancer: a machine learning, multicenter study. *EBioMedicine*. 2021;69:103460. https://doi.org/10.1016/j.ebiom.2021.103460.
27. Ouyang W, Jiang Y, Bu S, et al. A prognostic risk score based on hypoxia-, immunity-, and epithelialto-mesenchymal transition-related genes for the prognosis and immunotherapy response of lung adenocarcinoma. *Front Cell Dev Biol*. 2021;9:758777. https://doi.org/10.3389/fcell.2021.758777.
28. Huang Y, Ouyang W, Wang Z, et al. A comprehensive analysis of programmed cell death-associated genes for tumor microenvironment evaluation promotes precise immunotherapy in patients with lung adenocarcinoma. *J Personalized Med*. 2023;13:476. https://doi.org/10.3390/jpm13030476.
29. Yu Y, Chen H, Ouyang W, et al. Unraveling the role of M1 macrophage and CXCL9 in predicting immune checkpoint inhibitor efficacy through multicohort analysis and single-cell RNA sequencing. *MedComm*. 2020;2024:e471. https://doi.org/10.1002/mco2.471.
30. Xu S, Liu D, Chang T, et al. Cuproptosis-associated lncRNA establishes new prognostic profile and predicts immunotherapy response in clear cell renal cell carcinoma. *Front Genet*. 2022;13:938259. https://doi.org/10.3389/fgene.2022.938259.
31. Wang K, Zhong W, Long Z, et al. 5-Methylcytosine RNA methyltransferases-related long non-coding RNA to develop and validate biochemical recurrence signature in prostate cancer. *Front Mol Biosci*. 2021;8:775304. https://doi.org/10.3389/fmolb.2021.775304.
32. Jiang Z, Li J, Feng W, Sun Y, Bu J. A ferroptosis-related lncRNA model to enhance the predicted value of cervical cancer. *JAMA Oncol*. 2022;2022:6080049. https://doi.org/10.1155/2022/6080049.
33. Cheng B, Lai Y, Huang H, et al. MT1G, an emerging ferroptosis-related gene: a novel prognostic biomarker and indicator of immunotherapy sensitivity in prostate cancer. *Environ Toxicol*. 2024;39:927–941. https://doi.org/10.1002/tox.23997.
34. Peng S, Zhang X, Huang H, et al. Glutathione-sensitive nanoparticles enhance the combined therapeutic effect of checkpoint kinase 1 inhibitor and cisplatin in prostate cancer. *APL Bioeng*. 2022;6:046106. https://doi.org/10.1063/5.0126095.
35. Lee G, Kim CW, Choi JR, et al. Copper arsenite-complexed Fenton-like nanoparticles as oxidative stress-amplifying anticancer agents. *J Contr Release*. 2022;341:646–660. https://doi.org/10.1016/j.jconrel.2021.12.016.